



University of Groningen

## Bacterial replication, transcription and translation

Robinson, Andrew; van Oijen, Antoine M.

*Published in:*  
Nature Reviews Microbiology

*DOI:*  
[10.1038/nrmicro2994](https://doi.org/10.1038/nrmicro2994)

**IMPORTANT NOTE: You are advised to consult the publisher's version (publisher's PDF) if you wish to cite from it. Please check the document version below.**

*Document Version*  
Publisher's PDF, also known as Version of record

*Publication date:*  
2013

[Link to publication in University of Groningen/UMCG research database](#)

*Citation for published version (APA):*

Robinson, A., & van Oijen, A. M. (2013). Bacterial replication, transcription and translation: mechanistic insights from single-molecule biochemical studies. *Nature Reviews Microbiology*, 11(5), 303-315.  
<https://doi.org/10.1038/nrmicro2994>

### Copyright

Other than for strictly personal use, it is not permitted to download or to forward/distribute the text or part of it without the consent of the author(s) and/or copyright holder(s), unless the work is under an open content license (like Creative Commons).

### Take-down policy

If you believe that this document breaches copyright please contact us providing details, and we will remove access to the work immediately and investigate your claim.

Downloaded from the University of Groningen/UMCG research database (Pure): <http://www.rug.nl/research/portal>. For technical reasons the number of authors shown on this cover page is limited to 10 maximum.

# Bacterial replication, transcription and translation: mechanistic insights from single-molecule biochemical studies

Andrew Robinson and Antoine M. van Oijen

**Abstract** | Decades of research have resulted in a remarkably detailed understanding of the molecular mechanisms of bacterial DNA replication, transcription and translation. Our understanding of the kinetics and physical mechanisms that drive these processes forward has been expanded by the ability of single-molecule *in vitro* techniques, such as force spectroscopy and single-molecule Förster (fluorescence) resonance energy transfer (smFRET), to capture short-lived intermediate states in complex pathways. Furthermore, these technologies have revealed novel mechanisms that support enzyme processivity and govern the assembly of large multicomponent complexes. Here, we summarize the application of *in vitro* single-molecule studies to the analysis of fundamental bacterial processes, with a focus on the most recent functional insights that have been gained from fluorescence-based methods.

DNA replication, transcription and translation operate with astounding speed and fidelity in bacterial cells<sup>1</sup>. Moreover, regulation of these processes allows the rate of each to be adjusted according to changing environmental conditions<sup>2–4</sup>. Through extensive biochemical, genetic and structural analysis over the past 60 years, we have achieved a solid understanding of both the order of molecular events underlying these processes and many aspects of their regulation. We are approaching the point at which complete models can be made that accurately reflect each process in the cellular environment. What is currently missing, however, is information about the kinetics of molecular associations and conformational transitions, the natural variation in the rates of individual reaction steps and the potential existence of multiple parallel reaction pathways. A functional description of any one replisome, RNA polymerase (RNAP) molecule or ribosome, which might transiently change in behaviour (for example, by pausing) or carry out reactions at a slightly different rate to other molecules of the same type, is extremely difficult to extract using classical biochemical techniques, which for reasons relating to sensitivity, report only the average output of many molecules.

Recently, biophysicists have turned their attention to fundamental bacterial processes, attempting to link each step of a pathway with the physical processes that govern its operation. This has resulted in the development of

*in vitro* single-molecule techniques that can determine the activities of biomolecules, often in real time, with peerless precision and without a need for population averaging. Statistical analysis of single-molecule trajectories can pinpoint rate-limiting steps along reaction pathways and can reveal transient intermediates without the need for synchronization of the molecules in the reaction vessel. For processive events, such as DNA replication, transcription and translation, the single-molecule approach allows for direct observation of pausing events and variations in reaction rates from molecule to molecule<sup>5</sup>. Single-molecule studies are already making significant contributions to our understanding of these bacterial processes by providing access to important kinetic and physical parameters<sup>1,6</sup>.

Besides providing important quantitative information on previously known processes, the ability to follow complex multiprotein systems as they undergo a series of biochemical transitions has led to a number of novel mechanistic insights. The power of these technologies for the study of bacterial processes is reflected in the growing number of relevant research papers in the literature; however, a comprehensive overview of all these findings is beyond the scope of this Review. Here, we describe the principles of both force- and fluorescence-based single-molecule methods and highlight a number of recent examples in which *in vitro* single-molecule

Zernike Institute for  
Advanced Materials,  
University of Groningen,  
Groningen 9747 AG,  
The Netherlands.  
Correspondence to A.M.v.O.  
e-mail: [a.m.van.oijen@rug.nl](mailto:a.m.van.oijen@rug.nl)  
doi:10.1038/nrmicro2994  
Published online 3 April 2013

fluorescence techniques have provided novel insights relevant to how DNA replication, transcription and translation operate within the bacterial cell.

#### Techniques for *in vitro* single-molecule analysis

Single-molecule analysis requires that individual molecules be captured such that they are observable in isolation from other molecules, allowing any signal that is generated to be reliably ascribed to a single molecule. For *in vitro* experiments, molecules (typically nucleic acids or proteins) are usually separated from each other spatially by tethering the molecules at low density to a derivatized glass coverslip. Biochemical reactions, interactions and/or conformational changes can then be monitored by attaching either fluorescent dyes or beads to the molecule of interest and examining the dynamics of the molecule using microscopy. These techniques have been reviewed in detail elsewhere<sup>5,7</sup>. Here we provide only a brief summary to aid in understanding the physical basis of the experimental measurements discussed in later sections.

**Tethered-particle techniques.** Tethered-bead techniques are generally used to measure the activities of enzymes or proteins that change the properties of nucleic acids; such proteins include polymerases<sup>8</sup>, transcription factors<sup>9</sup> and nucleases<sup>10</sup>. Typically, one end of a nucleic acid molecule is attached to a glass surface, while the other end is attached to a bead. In one type of experiment, beads are tethered to the bottom surface of a flow cell. Reaction buffer is introduced by laminar flow, which in turn produces drag force on the beads, causing the DNA to stretch and the beads to pull close to the glass surface (TABLE 1). At low stretching forces (~3 piconewtons (pN)), single-stranded (ssDNA) collapses into compact ball-like structures, whereas double-stranded DNA (dsDNA) is more extended. Reactions that convert ssDNA to dsDNA or vice versa cause a change in the end-to-end length of the DNA, which is measured by monitoring the position of the bead over time. In an alternative method, no stretching force is applied, resulting in a surface-tethered DNA molecule for which the motions are determined solely by Brownian motion (TABLE 1). By tracking the lateral position of the bead attached to the end of the DNA at high temporal resolution, the end-to-end length of the molecule can be calculated and changes in length can be monitored over time. Tethered-bead experiments yield a lower spatial resolution than that achieved with other force-based techniques (see below), but can be used to measure the activities of hundreds of molecules in parallel and are primarily used for the detection of rare events.

More commonly, researchers probe the mechanical properties of polymers (typically nucleic acids) by force spectroscopy using optical tweezing or magnetic tweezing. These techniques allow measurements to be made at extremely high resolution, but measurements are obtained only one molecule at a time. In optical-tweezing experiments (TABLE 1), beads are often attached to both ends of the molecule of interest and one end is trapped in a focused laser beam<sup>11</sup>, whereas in magnetic-tweezing experiments (TABLE 1), the molecule is tethered to a glass

surface and the magnetic bead is attached to the free end. Moving or rotating the bead relative to the microscope stage (for example, using a suction pipette or a second optical trap in optical tweezing, and applying a magnetic field in magnetic tweezing (TABLE 1)) generates a pulling or twisting force, allowing the force-induced effects on biochemical reactions to be observed. Alternatively, the system can be used to study reaction-induced changes in the length of the nucleic acid by measuring the end-to-end distance between the beads (in optical tweezing) or between the magnetic bead and the glass surface (in magnetic tweezing). Using state-of-the-art tweezer devices, it is possible to measure changes in DNA length with single-base-pair resolution.

**Fluorescence techniques.** Fluorescence-based single-molecule techniques are used to measure molecular associations (for example, protein-protein or protein-DNA interactions) and conformational changes in biomolecules. Using a wide-field microscope equipped with a high-power laser source and a sensitive EMCCD camera (electron-multiplying charge-coupled device camera), or using a confocal microscope, it is possible to measure fluorescence arising from a single fluorophore molecule. Thus, labelling with a suitable fluorophore allows the direct observation of a surface-tethered molecule over an extended period of time. If differently coloured dyes are used, it is possible to observe multiple molecules simultaneously (TABLE 1). One of the main challenges associated with these techniques is photobleaching. However, because photobleaching is dependent on photon load and not time, excitation light can be applied in pulses when imaging over long periods (for example, during a time-lapse experiment) to extend the lifetime of the fluorophore.

Attaching two differently coloured dyes to a system of interest also allows single-molecule Förster (fluorescence) resonance energy transfer (smFRET) to be measured<sup>12</sup>. This approach facilitates the real-time measurement of dye-to-dye distances of up to ~5 nm. If the dyes are attached to different molecules (for example, one to DNA and the other to an interacting protein), association events and relative movements of the molecules can be detected (TABLE 1). Alternatively, both dyes can be placed at different sites on the same molecule, which allows conformational changes within a single molecule to be observed. Use of smFRET requires that the overall structure of the molecule or complex of molecules is well defined and that suitable means for site-specific attachment of fluorophores are available.

#### DNA replication

**Assembly of the replisome.** In most bacteria, DNA replication is initiated at a single site on the circular chromosome, known as the origin of replication (*oriC* in *Escherichia coli*), which is recognized and unwound by the initiator protein, DnaA<sup>13</sup> (FIG. 1). On the basis of crystal structures of a truncated form of *Aquifex aeolicus* DnaA, it was proposed that DnaA forms extended right-handed filaments that stretch the origin DNA to facilitate unwinding<sup>14</sup>. Recent single-molecule magnetic-tweezer

#### Derivatized glass coverslip

A microscope coverslip that has been coated or chemically treated to allow site-specific attachment of biomolecules.

#### Flow cell

A microscopy sample environment that allows liquid flow over surface-immobilized particles.

#### Drag

A force that acts on solid objects placed in a liquid flow. Drag acts in the same direction as the flow.

#### Brownian motion

Random movement of particles in suspension, resulting from bombardment by solvent molecules.

#### EMCCD camera

(Electron-multiplying charge-coupled device camera). A camera that can be used to capture low-level light emanating from a microscopy sample, for example.

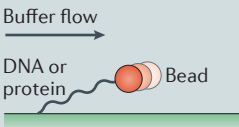
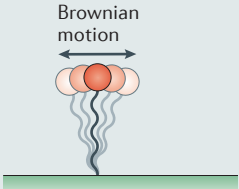
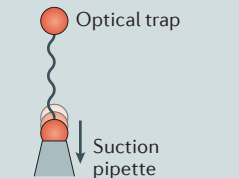
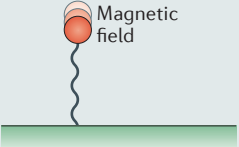
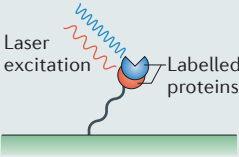
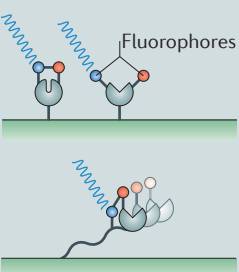
#### Fluorophore

A compound that is capable of producing fluorescence, such as an organic dye or a fluorescent protein.

#### Förster (fluorescence) resonance energy transfer

A phenomenon whereby energy induced by light excitation is transferred from one fluorophore to another in a distance-dependent manner.

Table 1 | Single-molecule *in vitro* techniques that can be used to study biochemical reactions

Technique	Principle	Advantages	Challenges	Hardware	Applications
<i>Force-based techniques (used to measure changes in the properties of single nucleic acid molecules during biochemical reactions)</i>					
<p>Flow stretching of tethered particles</p> 	<p>Beads are tethered to the surface of a flow cell by single molecules of DNA or RNA; reaction buffer is pulled through by suction, causing drag force on the beads</p>	<p>Highly parallel measurements; well suited for detecting rare events</p>	<p>Moderate resolution (DNA length changes of ~100 bp can be measured)</p>	<p>A standard inverted microscope with a CCD camera</p>	<p>Measuring the rates of action of individual DNA polymerase<sup>26</sup> and exonuclease<sup>10</sup> molecules</p>
<p>Tethered-particle motion</p> 	<p>No stretching force is applied, bead movements are determined solely by Brownian motion</p>	<p>Highly parallel measurements; well suited for detecting rare events</p>	<p>Moderate resolution (DNA length changes of ~100 bp can be measured)</p>	<p>A standard inverted microscope with a CCD camera</p>	<p>Measuring DNA looping induced by the binding of transcription factors<sup>9</sup></p>
<p>Force spectroscopy with optical tweezers</p> 	<p>Beads are attached to both ends of a DNA or RNA molecule; one bead is trapped using a focused laser beam, and the other is manipulated using a mechanically controlled suction pipette or second optical trap, which is moved away from the first bead to impart stretching force</p>	<p>High resolution</p>	<p>Low data throughput; requires specialist equipment</p>	<p>An optical-tweezer device</p>	<p>Measuring the rates of translating ribosomes<sup>80</sup></p>
<p>Force spectroscopy with magnetic tweezers</p> 	<p>A magnetic bead is tethered to a surface by a single molecule of DNA or RNA; moving or rotating the bead relative to the microscope stage using an applied magnetic field generates pulling or twisting force</p>	<p>High resolution</p>	<p>Low data throughput; requires specialist equipment</p>	<p>A magnetic-tweezer device</p>	<p>Measuring DNA dynamics during transcription<sup>41</sup>; probing the structural properties of DNA-protein complexes<sup>15</sup></p>
<i>Fluorescence-based techniques (used to measure protein-protein or protein-DNA interactions and conformational changes in biomolecules)</i>					
<p>Multiwavelength fluorescence microscopy</p> 	<p>Molecules are labelled at specific sites (for example, Cys residues) with suitable fluorophores; molecules that are tethered to surfaces (either directly or through interaction with a directly tethered molecule) diffuse slowly and are detected as foci, whereas unbound molecules move quickly through solution and thus produce a diffuse (background) fluorescence signal</p>	<p>Direct observation of multiple surface-tethered molecules over extended periods of time</p>	<p>Photobleaching is caused by the necessarily high excitation power</p>	<p>An inverted fluorescence microscope with high-power laser excitation and an EMCCD camera</p>	<p>Visualizing the real-time assembly of ribosomes<sup>57</sup>; observing tRNA movements on ribosomes during translation<sup>60</sup></p>
<p>smFRET</p> 	<p>Two different fluorophores are attached to the molecule of interest; if the emission band of one (the donor) overlaps with the excitation band of the other (the acceptor) and the fluorophores lie within a certain distance of each other (typically ~5 nm), FRET will occur, wherein the donor fluorophore transmits energy to the acceptor fluorophore<sup>12</sup></p>	<p>Dynamic observation of molecular interactions and conformational changes</p>	<p>Requires detailed prior knowledge of biomolecular structures</p>	<p>An inverted fluorescence microscope with high-power laser excitation and an EMCCD camera, or a confocal microscope</p>	<p>Monitoring the real-time formation of transcription complexes<sup>81</sup>; observing conformational changes in RNA polymerase molecules<sup>47</sup>; monitoring tRNA transit in active ribosomes<sup>12</sup></p>

CCD, charge-coupled device; EMCCD, electron-multiplying CCD; smFRET, single-molecule Förster (fluorescence) resonance energy transfer.

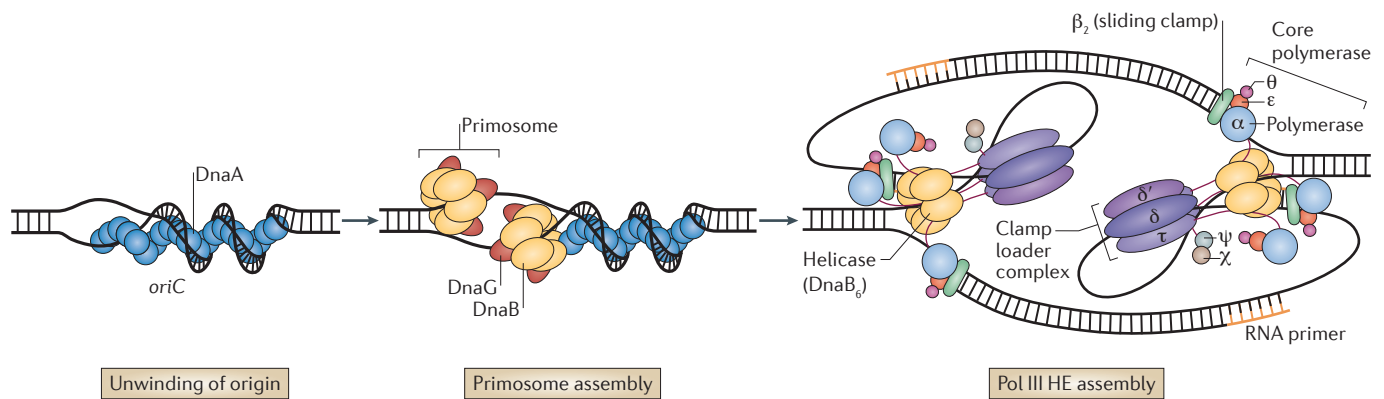


**Figure 1 | Initiation of DNA replication in *Escherichia coli*.** During the initiation stage of DNA replication, double-stranded DNA within the origin of replication (*oriC*) is melted through the action of the initiator protein, DnaA, generating single-stranded DNA substrates for replication. The primosome (DnaB<sub>6</sub>-DnaG<sub>3</sub>) and DNA polymerase III holoenzyme (Pol III HE) complexes are assembled at the melted origin and together proceed bidirectionally around the circular chromosome. The exact pathways for assembly of the *E. coli* primosome and Pol III HE complexes are not yet known, but single-molecule Förster (fluorescence) resonance energy transfer studies have shown that in the bacteriophage T4 replication system, the primosome is assembled through hierarchical association of each component, whereas Pol HE can be assembled through multiple pathways (see BOX 1).

measurements support this model and show that full-length *E. coli* DnaA forms stable, right-handed helical filaments of variable length on DNA containing an *oriC* sequence<sup>15</sup>.

When the parental DNA strands are separated, the replicative helicase (DnaB in *E. coli*) and DNA primase (DnaG in all bacteria) are loaded to form the primosome complex (with a ratio DnaB<sub>6</sub>/DnaG<sub>3</sub> in *E. coli*) (FIG. 1). Within this complex, the helicase unwinds the parental DNA strands, and the primase synthesizes short RNA primers, one for the leading strand and one for each of the ~4,000 Okazaki fragments synthesized on the lagging strand during the course of a DNA replication cycle<sup>16</sup>. The mechanisms governing the assembly of primosomes are not well understood, and disparate proteins are known to be involved across the different bacterial phyla<sup>17-19</sup>. Current models for primosome assembly, which are based on the work of many research groups using data generated by a wide range of different techniques, suggest that there are significant mechanistic differences between bacteria<sup>19</sup>. Recent work has shown, however, that it is possible to directly follow the assembly of primosome complexes *in vitro* using smFRET<sup>20</sup>. In this study, the primosome complex of the bacteriophage T4 was observed to assemble through a single hierarchical pathway (BOX 1). This approach could now be used to observe the assembly of bacterial primosomes.

After the first RNA primer is synthesized, the primary replication enzyme — DNA polymerase III holoenzyme (Pol III HE) in bacteria — is assembled (FIG. 1). Pol III HE is a multisubunit enzyme containing three major working parts: the core polymerases (each comprising an  $\alpha$ -subunit, an  $\epsilon$ -subunit and a  $\theta$ -subunit), which provide polymerase and proof-reading activities; the sliding clamps (each comprising two  $\beta$ -subunits and called  $\beta_2$ ), which enable processive DNA synthesis; and a clamp loader complex (comprising three

$\tau$ -subunits, a  $\delta$ -subunit, a  $\delta'$ -subunit, a  $\chi$ -subunit and a  $\psi$ -subunit, collectively called  $\tau_3\delta\delta'\chi\psi$ ), which both loads the  $\beta_2$  clamps on and removes them from the DNA, as well as tethering three core polymerases (see below). The assembly pathway of these components at a primer terminus has not yet been determined for any bacterial system; however, assembly of the analogous T4 Pol HE has been observed using smFRET, and in contrast to primosome assembly, the process was found to be non-hierarchical<sup>21</sup> (BOX 1).

**Coordination of leading-strand and lagging-strand synthesis.** Following assembly on a primed template, Pol III HE is highly processive. In fluorescence assays, single molecules of *E. coli* Pol III HE were found to replicate 85 kb of DNA on average, at an average rate of ~500 bp per second<sup>22</sup>. Each core polymerase (of which there are three in Pol III HE) can synthesize DNA only in the 5'-to-3' direction. Because DNA is antiparallel, this means that only one strand, called the leading strand, can be synthesized continuously. On the other, so-called lagging strand, DNA is synthesized discontinuously as Okazaki fragments, in the opposite direction to that of helicase movement. Single-molecule flow-stretching assays with the T7 bacteriophage Pol HE system demonstrated that a loop is formed on the lagging strand in order to solve this direction problem and maintain coordination between the leading-strand and lagging-strand polymerases<sup>8</sup> (BOX 1).

In *E. coli*, synthesis of each primer on the lagging strand takes ~1 second<sup>23</sup>. It is not clear whether the helicase, to which the primase is bound, pauses during primer synthesis or keeps moving forward. In separate single-molecule studies using magnetic tweezers (with T4 Pol HE) and smFRET (with T7 Pol HE), evidence was found for a second lagging-strand loop, formed between the helicase and the primase<sup>24,25</sup>. This primer

#### Okazaki fragments

Regions of double-stranded DNA that are produced during discontinuous synthesis of the lagging strand.

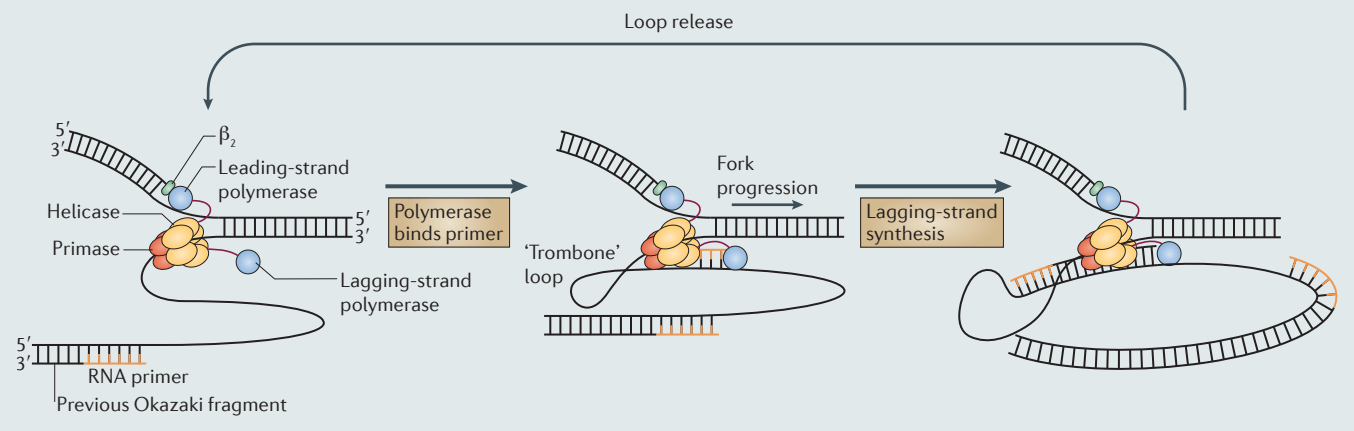
## Box 1 | Single-molecule studies of bacteriophage replisomes

In bacteria, DNA replication requires at least 15 proteins. Because of this complexity, the related but simplified replication systems of the bacteriophages T4 and T7 have often been used as models for the bacterial replication machinery. The T4 replisome consists of eight proteins, which together form similar working parts to those used in bacterial replication: a DNA polymerase (gp43), a clamp loader complex (gp44 and gp62), a processivity clamp (gp45), a single-stranded DNA-binding protein (SSB; gp32), a primase (gp61), a helicase (gp41) and a helicase loader (gp59)<sup>21</sup>. The T7 system is even simpler, comprising only a polymerase (gp5), a combined helicase–primase (gp4) and an SSB (gp2.5)<sup>30</sup>. The *Escherichia coli* host protein thioredoxin is bound by the T7 polymerase and used as a processivity factor<sup>78</sup>. Single-molecule experiments have revealed key aspects of the T4 and T7 replication mechanisms that are likely to be conserved in bacteria.

In one study, the assembly of the T4 primosome complex at forked DNA was monitored using single-molecule Förster (fluorescence) resonance energy transfer (smFRET)<sup>20</sup>. In this study, assembly was achieved through hierarchical recruitment of SSB, the helicase loader, the helicase and, finally, the primase to the forked DNA substrate. In a follow-up study, the same smFRET approach was used to monitor the assembly of the T4 DNA polymerase holoenzyme<sup>21</sup>. Interestingly, functional complexes could be formed on the forked DNA through four alternative pathways. In the first pathway, the clamp and clamp loader bind as a complex, followed by the polymerase; in the second and third pathways, either the clamp loader or

the clamp, respectively, binds first, and the polymerase is the last component to assemble; and in the fourth pathway, the polymerase assembles first, followed by the clamp and then the clamp loader. A similar smFRET approach or a multiwavelength fluorescence microscopy approach could be applied to monitor assembly of the bacterial Pol III HE system.

In another single-molecule study, the directionality problem in replication was addressed. DNA is antiparallel, but DNA polymerases can synthesize DNA only in the 5′-to-3′ direction. It has long been assumed that loops must periodically form on the lagging strand so that DNA synthesis can progress in the opposite direction to that of helicase movement, without disrupting leading-strand synthesis (see the figure)<sup>79</sup>. Forty years after this was first proposed, flow-stretching assays with the T7 DNA polymerase holoenzyme provided the first direct observation of lagging-strand loops in active replisomes<sup>8</sup>. By analysing loop sizes and lag times between loops, two mechanisms for the release of these loops were identified. In the first scenario, collision of the lagging-strand polymerase with an upstream Okazaki fragment triggers polymerase dissociation from the DNA, resulting in release of the loop. In the second scenario, the new primer that is synthesized downstream of the lagging-strand polymerase triggers dissociation of the polymerase through an as-yet-unidentified intersubunit signalling mechanism. From the single-molecule data, it became clear that both mechanisms are at play during T7 replication: half of the loop release events could be attributed to collisional release, and the other half to signalled release.



loop mechanism would allow the helicase to keep moving during primer synthesis. On the other hand, single-molecule flow-stretching experiments have demonstrated that leading-strand synthesis pauses during primer synthesis in the T7 system, suggesting that the helicase pauses during this time<sup>26</sup>. Further work is needed to understand these apparent discrepancies.

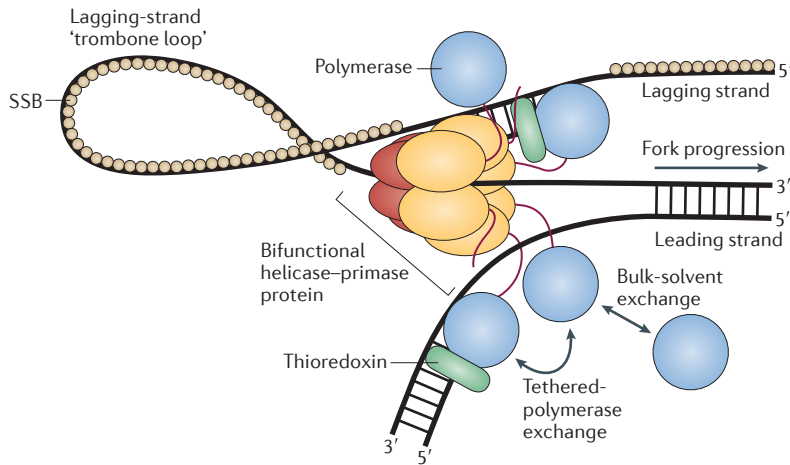
#### Stably bound but exchangeable replisome components.

The clamp loader and the core polymerases are held together by strong interactions between the  $\tau$ -subunits of the clamp loader and the  $\alpha$ -subunits of the core polymerases; the  $\tau$ -subunit– $\alpha$ -subunit interaction has a dissociation constant ( $K_D$ ) of  $\sim 260$  pM<sup>27</sup>. In light of this strong contact between the clamp loader and the core polymerases, and the high processivity of Pol III HE, it is generally assumed that the core polymerases of Pol III HE remain stably attached to the clamp loader during coordinated synthesis on the leading and lagging strands. However, recent single-molecule data challenge this assumption. By monitoring the fluorescence

intensity of replisome markers inside live *E. coli* cells, compelling evidence has been obtained for the regular exchange of core polymerases on the lagging strand<sup>28</sup> (FIG. 2). On the basis of this data, it has been proposed that the lagging-strand core polymerase is exchanged when each Okazaki fragment is produced and also that the lagging-strand core polymerase synthesizes DNA for only half the time of an Okazaki fragment cycle, but it therefore does so at a faster rate than the leading-strand core polymerase. These findings have yet to be confirmed in a more rigorous *in vitro* study, but an appropriate single-molecule assay has already been developed to visualize polymerase exchange in the T7 Pol HE system<sup>29</sup> (BOX 1).

By combining flow stretching, to visualize DNA synthesis, with fluorescence labelling of T7 polymerase subunits to monitor their binding to DNA, it was found that the leading-strand polymerase also undergoes regular exchange (on average, every 50 seconds) with available polymerases in solution<sup>29</sup>. Interestingly, earlier ensemble measurements of DNA synthesis showed

**a T7 replication fork**



**b Escherichia coli replication fork**

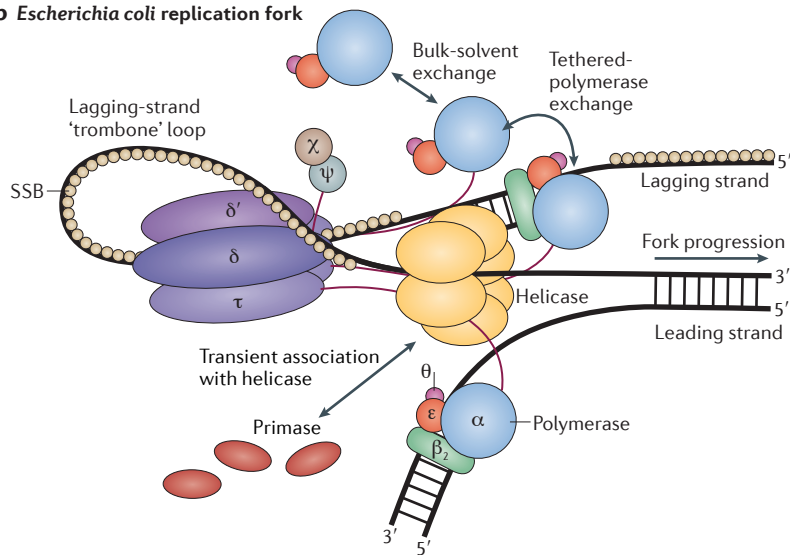


**Figure 2 | Mechanism of core-polymerase exchange in the T7 and *Escherichia coli* systems.** During DNA synthesis, both T7 DNA polymerase holoenzyme (Pol HE) and *Escherichia coli* Pol III HE can undergo exchange of the polymerase subunits while simultaneously remaining attached at the replication fork. **a** | In the T7 system, the leading-strand and lagging-strand polymerases are tethered to the helicase–primease complex through an acidic carboxy-terminal tail present on each of the six helicase subunits<sup>30</sup>. If either the leading-strand or lagging-strand polymerase dissociates from the DNA, there is a high local concentration of this polymerase owing to the tether, and the polymerase can quickly rebind. If excess polymerase is present in bulk solution, all six binding sites on the helicase can become occupied. Thus, if the leading-strand or lagging-strand polymerase dissociates, there is a chance that it will be replaced by one of the competing polymerases bound to the helicase, which are held in similarly high local concentrations. **b** | Analogous anatomy is found in *E. coli* Pol III HE<sup>28,30</sup>, in which each of the three  $\tau$ -subunits in the clamp loader complex contains a binding site for a core polymerase (each of which contains an  $\alpha$ -subunit with polymerase activity, an  $\epsilon$ -subunit and a  $\theta$ -subunit). This probably facilitates exchange through a similar mechanism to that used in the T7 system. SSB, single-strand-DNA-binding protein.

weak interactions that tether each T7 polymerase to a carboxy-terminal domain in the hexameric helicase (which can bind up to six polymerases)<sup>30</sup>. If the leading-strand polymerase dissociates from the fork in the absence of competing polymerases, it remains tethered to the helicase, ensuring a high local concentration of the polymerase and thus facilitating rapid rebinding to the fork (FIG. 2a). By contrast, in the presence of excess polymerases, the six C termini of the helicase are occupied with competing polymerases, producing a high local concentration of potential replacement polymerases at the fork. Thus, if the replicating polymerase dissociates, it can be replaced by one of the competing polymerases. Given that the *E. coli* Pol III HE shows analogous behaviour — that is, core polymerases are stably bound in the absence of other core polymerases in solution<sup>22</sup>, but are exchanged on the lagging strand *in vivo* when core polymerases are in excess<sup>28,31</sup> — it seems likely that a similar mechanism is at play in bacteria (see below).

**Architecture of the DNA polymerase III holoenzyme.**

A key issue relating to this process of core polymerase exchange concerns the architecture of Pol III HE at the replication fork. Within Pol III HE, the three core polymerases are tethered together by the clamp loader complex, which contains seven subunits, three of which are encoded by *dnaX*. *E. coli dnaX* encodes two products: the full-length  $\tau$ -subunit and a shorter  $\gamma$ -subunit arising from a programmed translational frameshift. Each  $\tau$ -subunit is capable of tethering one core polymerase, whereas the  $\gamma$ -subunit lacks this function. Whereas purified preparations of Pol III HE typically contain two  $\tau$ -subunits and one  $\gamma$ -subunit, reconstitution of clamp loader complexes from mixtures containing both proteins overwhelmingly yields  $\tau_3\delta\delta'\chi\psi$  and  $\gamma_3\delta\delta'\chi\psi$  complexes<sup>32</sup>. Furthermore, recent *in vivo* single-molecule studies indicate that the active form of Pol III HE at replication forks contains three  $\tau$ -subunits and, thus, three core polymerases<sup>28,31</sup>. The reason for these discrepancies is not yet clear, and a satisfactory explanation will probably require additional *in vivo* studies<sup>33</sup>.

Importantly, however, a single-molecule fluorescence study revealed a clear difference in the activities of *E. coli* Pol III HEs containing two, as opposed to three, core polymerases<sup>34</sup>. DNA molecules were captured in a DNA curtain<sup>35</sup> for use as substrates for rolling-circle replication. Under these conditions, the Pol III HE variant containing two core polymerases showed a significantly lower processivity than Pol III HE containing three core polymerases, and the products of the former variant contained many more single-stranded DNA gaps<sup>34</sup>. These observations imply that Pol III HE containing three core polymerases is much more efficient at lagging-strand synthesis than the variant that contains only two, as this variant seems to often fall off the template before completing an Okazaki fragment. Although it might seem unnecessary for an enzyme charged with copying two strands of DNA to contain three core polymerases, this study shows that such an arrangement affords a clear advantage. An interesting possibility is that the availability of three core polymerases provides Pol III HE with

that in the absence of free polymerase in solution, the leading-strand polymerase remains closely associated with the replication fork<sup>30</sup>. This ability to remain tightly associated with the fork but undergo exchange when challenged with free polymerase arises from the

access to the stable-yet-exchangeable mechanism of polymerase binding described for T7 Pol HE (see above). In this mechanism, if one core polymerase dissociates from the template, it could be quickly replaced by the third, 'spare' core polymerase, which is present at a high local concentration owing to tethering at the fork by the  $\tau$ -subunit (FIG. 2b). This hypothesis should now be put to the test *in vitro* and could be assessed using a mixture of differently labelled polymerase molecules. If found to be true, such a mechanism might confer an advantage in the cellular environment by providing a means for the cell to replace poorly-functioning polymerases with newly synthesized versions, without interrupting DNA synthesis. An interesting further possibility is that one or more alternative polymerases (for example, Pol II, Pol IV or Pol V) also gain access to the replication fork using this exchange mechanism.

In the cellular environment, replication forks frequently encounter transcribing RNAP molecules or DNA lesions, both of which hinder the replication fork and can result in fork arrest and cell death<sup>36</sup>. One mechanism by which Pol III HE can circumvent these blockages involves a core polymerase 'hopping' from behind the blockage to a sliding clamp loaded at a newly synthesized primer upstream<sup>37</sup>. The core polymerase does this without dissociating from the fork. In light of strong support for the three-core-polymerase architecture of Pol III HE, an alternative mechanism is possible. The 'spare' core polymerase could potentially bind to the newly placed clamp before the blocked core polymerase is released, allowing the Pol III HE to 'step' over the blockage. An advantage of this mechanism would be that two contacts with the template are maintained at all times, increasing the stability of Pol III HE at the blocked fork. Single-molecule experiments comparing the ability of two- and three-core-polymerase variants to bypass replication blockages could be used to distinguish between hopping and stepping mechanisms.

### Transcription

Recently, single-molecule techniques have been used to visualize the movements of RNAP on the template DNA in real time, which has provided kinetic information for almost every step of the transcription cycle<sup>38,39</sup>. In the past two years, exciting progress has been made towards understanding the assembly of initiation complexes, the conformational movements made by RNAP in the course of a transcription cycle and the physical principles underpinning the regulation of transcription initiation.

**Formation of the initiation complex.** Bacterial transcription, which has been studied almost exclusively in the *E. coli* model system, is commonly divided into three distinct phases: initiation, elongation and termination<sup>2</sup>. During initiation, RNAP binds to a promoter specificity determinant ( $\sigma$ -factor) to form an RNAP holoenzyme (RNAP HE). Bacteria typically produce several different  $\sigma$ -factors; accordingly, a number of RNAP HES with varying affinities for different promoters are generated. The cellular levels and activities of the different

$\sigma$ -factors change in response to environmental triggers, leading to large-scale changes in the gene expression profile of the cell. When RNAP HE initially binds to a promoter, the DNA remains double stranded. This state is termed the closed complex. RNAP HE then separates the DNA strands to form an open complex and uses one of the DNA strands as a template to synthesize mRNA (FIG. 3a). Single-molecule studies have revealed that RNAP HE initially remains bound at the promoter and scrunches the DNA template, which involves pulling in short stretches of the ssDNA template while remaining associated with the promoter region, producing a series of short abortive transcripts<sup>40,41</sup>. Eventually, RNAP HE clears the promoter and enters a highly processive elongation stage, translocating primarily using a Brownian ratchet mechanism<sup>42,43</sup> (FIG. 3b).

In a recent single-molecule fluorescence study, the entire initiation process was visualized at a  $\sigma^{54}$ -dependent promoter<sup>44</sup>.  $\sigma^{54}$ -RNAP HE is an alternative  $\sigma$ -factor complex produced in response to particular environmental conditions, most notably during nitrogen starvation. This RNAP HE differs in mechanism from the 'housekeeping'  $\sigma^{70}$ -RNAP HE in its requirement for binding to the activator protein NtrC in order to form the open complex. Thus, when studying this system *in vitro*, it is possible to stall the process at the closed-complex stage by omitting NtrC. It is also possible to stall at the open-complex stage by omitting substrate (NTPs), which prevents mRNA synthesis. By labelling the DNA template,  $\sigma^{54}$  and the transcript with different fluorescent dyes, it was possible to measure each of the kinetic steps involved in the initiation process<sup>44</sup> (summarized in FIG. 3a). This study found that two different closed complexes are formed, one that is short-lived (with a lifetime of ~2 seconds), and one that is longer-lived (with a lifetime of ~80 seconds). Both types of closed complex are formed many times before the open complex is formed, indicating that RNAP HE repeatedly binds to and dissociates from the promoter before transcription is initiated. NtrC-ATP associates with RNAP HE in the longer-lived closed state and, following hydrolysis of ATP, triggers the formation of the open complex. This opening of the DNA strands was found to be the rate-limiting step in the initiation process and represents the formation of an RNAP HE that is committed to a transcription cycle. Previous single-molecule studies showed that in some  $\sigma^{70}$ -RNAP HE transcription cycles,  $\sigma^{70}$  remains associated with RNAP, whereas in others, the  $\sigma$ -factor dissociates when RNAP enters the elongation phase<sup>45</sup>. For transcription mediated by  $\sigma^{54}$ -RNAP HE, however, in almost all events  $\sigma^{54}$  was found to dissociate when RNAP clears the promoter<sup>44</sup>. The initiation mechanism observed here provides novel insight for the regulation of  $\sigma^{54}$ -dependent genes in the cellular environment. The fact that formation of the open complex represents a commitment to productive transcription suggests that regulation of initiation must occur before this step. The transient, concentration-dependent binding of  $\sigma^{54}$ -RNAP HE to the promoter, as observed at the start of the pathway, would allow RNAP HE complexes to rapidly sample the promoter before committing

#### DNA curtain

A tethered-particle technique in which DNA molecules are trapped along a diffusion barrier within a flow cell and stretched parallel to the glass surface by drag.

#### Rolling-circle replication

A mode of DNA replication of a circular substrate to yield a linear, double-stranded product of theoretically infinite length.

#### Brownian ratchet

In the context of this article: a mechanism whereby particles undergoing Brownian motion are driven in a certain direction by selecting for only those motions that occur in the desired direction.



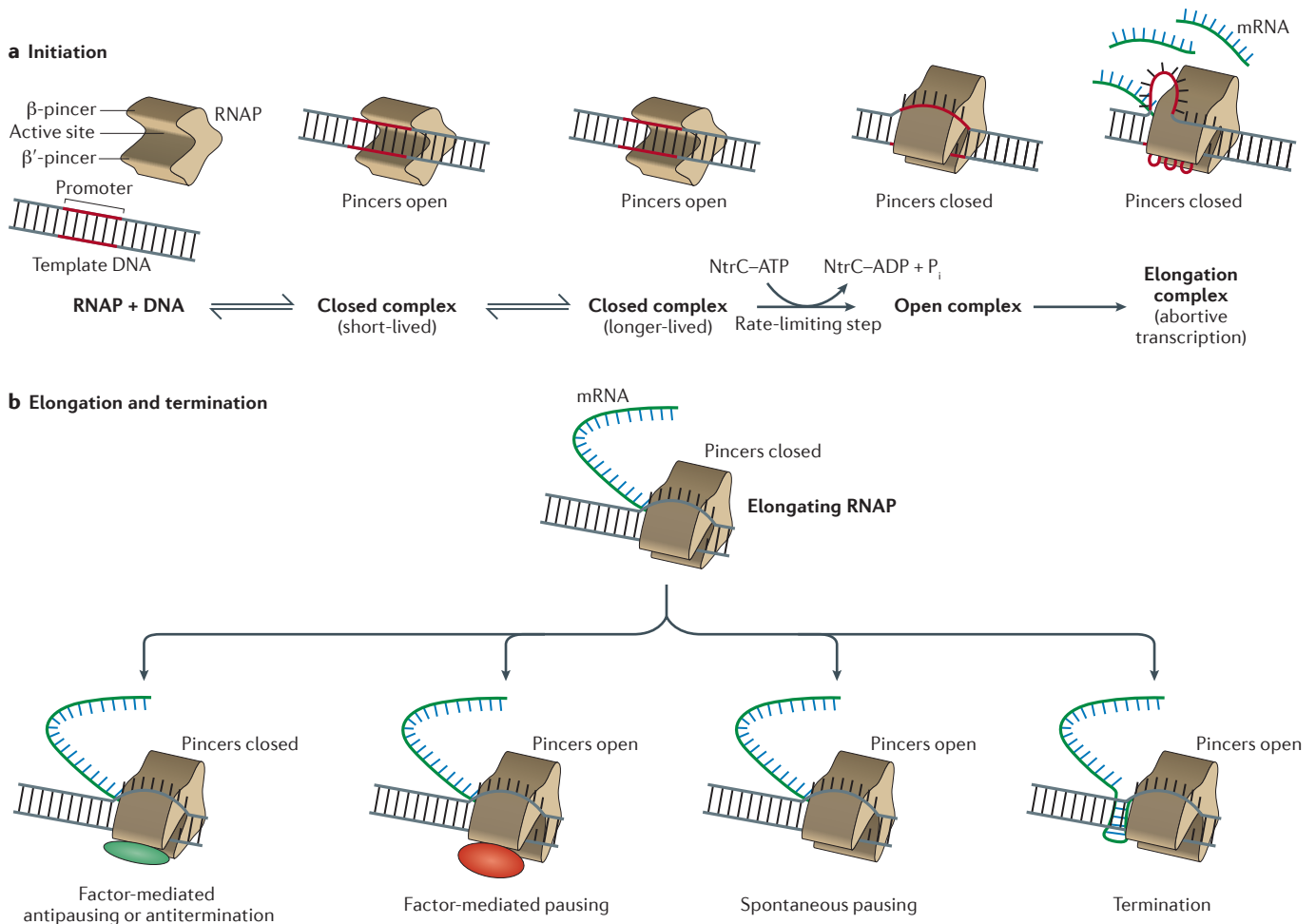


**Figure 3 | Binding and conformational changes of RNA polymerase during transcription at a  $\sigma^{54}$ -dependent promoter.** **a** | Initiation of transcription follows a well-defined pathway that is rate limited at the stage of open-complex formation<sup>45</sup>. Before open-complex formation, RNA polymerase holoenzyme (RNAP HE) and the associated promoter region fluctuate between a short-lived and a longer-lived closed-complex state, in which the  $\beta$ -pincer and  $\beta'$ -pincer are open and accommodate double-stranded DNA. Both  $\sigma^{54}$ -bound RNAP ( $\sigma^{54}$ -RNAP HE) and  $\sigma^{70}$ -RNAP HE exist primarily in an open pincer conformation (which corresponds to a closed complex) during the early stages of initiation<sup>47</sup>. When the open complex is formed, the  $\beta$ -pincer and  $\beta'$ -pincer close, latching RNAP HE onto the single-stranded DNA template. The clamp remains closed during abortive initiation and elongation. **b** | It is hypothesized that pauses in transcription (which can occur spontaneously or can be induced by certain transcription factors), as well as the process of transcription termination, coincide with re-opening of the RNAP HE pincers.

to transcription. This activity might be an important mechanism for altering the transcriptional profile of the cell, especially when changes in environmental conditions lead to a change in the  $\sigma$ -factor pool.

**Processive elongation and pausing by RNAP HE.** Until recently, single-molecule studies of transcription had focused on the movements of RNAP HE relative to the DNA template<sup>38,39</sup>, or unwinding of the template during open-complex formation<sup>46</sup>. In a recent smFRET study, conformational changes in RNAP HE were measured, and together with existing crystal structure data, these measurements provide a dynamic model of RNAP HE structure throughout the transcription cycle<sup>47</sup>. The structure of RNAP HE is reminiscent of a crab's claw<sup>48</sup>; the template DNA is surrounded by the so-called pincers formed by

the  $\beta$ -subunit and  $\beta'$ -subunit (FIG. 3). The RNAP HE active site is located at the base of the molecule, between the pincers. Crystal structures have revealed a series of different  $\beta'$ -pincer conformations, which correspond to open and closed forms as well as partially closed intermediates. In the smFRET study, analysis of both  $\sigma^{70}$ -RNAP HE and  $\sigma^{54}$ -RNAP HE in the absence of template revealed pincer conformations consistent with an open form (wide enough to accommodate dsDNA, such as in the closed RNAP HE–DNA complex) and a closed form (wide enough to accommodate ssDNA, such as in the open RNAP HE–DNA complex), as well as a novel collapsed form (which could not accommodate either ssDNA or dsDNA)<sup>47</sup>. In the presence of template dsDNA,  $\sigma^{70}$ -RNAP HE readily forms an open promoter complex, and only the closed conformation of the  $\beta'$ -pincer is observed.

This conformation persists as the reaction is allowed to proceed through the abortive initiation and elongation stages. In the case of  $\sigma^{54}$ -RNAP HE, it was possible to stall the system at the closed-complex stage by omitting the activator protein NtrC or using non-hydrolysable ATP analogues to prevent  $\sigma^{54}$ -RNAP HE–NtrC complexes from progressing past open-complex formation. In all the closed promoter complexes, the open form of the RNAP pincer was dominant. When the reaction was allowed to proceed to the open promoter complex stage by the addition of NtrC and ATP, only the closed  $\beta'$ -pincer was observed. These observations again show that as soon as the open promoter complex is formed, the RNAP HE pincers clamp tightly to the ssDNA template. The authors propose that the pincer-closed conformation of RNAP HE represents the active state of the enzyme and that commonly observed pauses during the elongation phase, as well as the process of termination, might coincide with re-opening of the pincers (FIG. 3b). Consistent with this proposed pausing mechanism, transcription factors that are known to increase or inhibit transcriptional pausing bind to RNAP at sites that would be predicted to favour the open or closed pincer conformations, respectively<sup>49,50</sup>. These hypotheses are now readily testable using the same smFRET platform.

### Translation

The basic mechanism of translation in bacteria is reasonably well understood: the main biochemical steps have been deduced, the overall kinetics of the process have been measured, and representative crystal structures of the bacterial ribosome have been captured at almost every step of the process<sup>6</sup>. Time-resolved single-molecule studies are now adding more detailed kinetic information to the picture, revealing previously unknown reaction intermediates and rates, conformational changes and association–dissociation events. The physical mechanisms that drive each step in the reaction forward are also being established. These topics have been reviewed in detail elsewhere<sup>6,51,52</sup>, so here we discuss two very recent single-molecule studies, which reveal that events in translation can occur through multiple pathways.

**Monitoring the dynamics of initiation.** There are three main binding sites for tRNAs on the bacterial ribosome: the A-site (acceptor site), the P-site (peptidyl site) and the E-site (exit site)<sup>6</sup>. During the initiation stage of translation, an initiator tRNA, known as fMet-tRNA (which carries the amino acid *N*-formylmethionine (fMet), the first amino acid of almost all bacterial proteins), binds at the P-site of the 30S ribosomal subunit, which is itself bound to a template mRNA<sup>53</sup> (FIG. 4a). A 50S subunit is then recruited to form the functional 70S ribosome. The assembly process is guided by three initiation factors known as translation initiation factor 1 (IF1), IF2 and IF3. IF2 in complex with GTP facilitates the correct binding of fMet-tRNA to the ribosomal P-site, and IF1 and IF3 regulate the binding of IF2–GTP to ensure that fMet-tRNA is matched with the correct start codon<sup>3</sup>. Historically, it was thought that IF2 bound fMet-tRNA and escorted it to the 30S subunit; however, recent

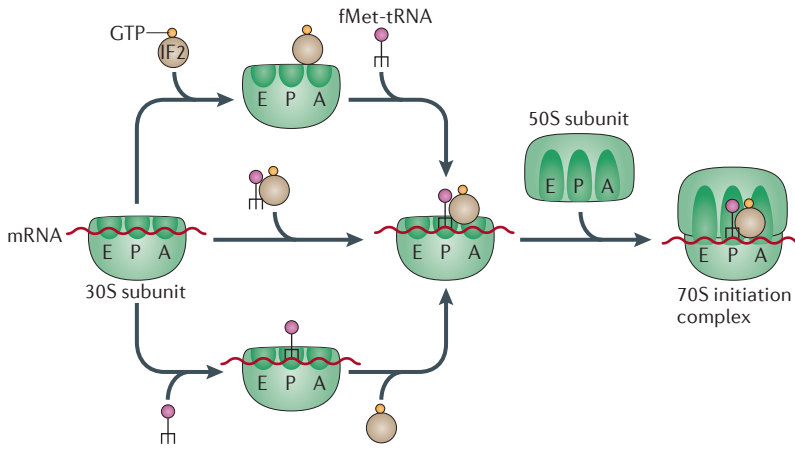
kinetic measurements suggest that IF2 binds to the 30S subunit first and subsequently recruits fMet-tRNA<sup>54–56</sup>.

The assembly of ribosome initiation complexes was recently examined by two groups, one using single-molecule fluorescence<sup>57</sup> and the other using bulk-phase FRET measurements<sup>55</sup> to observe the entire initiation process in real time. Using four different fluorescent dyes, the first group monitored the binding of labelled IF2–GTP, fMet-tRNA and 50S subunit to a labelled 30S subunit that was pre-loaded with template mRNA. They observed that the 70S ribosome could be formed by three alternative assembly pathways (FIG. 4a). In the first pathway, which was observed in 30% of their measurements, IF2–GTP binds the 30S subunit first, followed by fMet-tRNA and, last, the 50S subunit. In the second pathway, seen in 65% of their measurements, fMet-tRNA binds the 30S subunit first, followed by IF2–GTP and then the 50S subunit. Finally, in the third pathway, which was observed in 5% of cases, simultaneous binding of IF2–GTP and fMet-tRNA occurred, followed by 50S subunit binding. The addition of IF1 and IF3 to the reaction increased the proportion of IF2–GTP-first events and reduced the proportion of tRNA-first events, consistent with existing models which posit that IF1 enhances the binding of IF2 to the 30S subunit and prevents fMet-tRNA from binding at the incorrect tRNA-binding site on the 30S subunit<sup>3</sup>. Increasing the concentration of both IF2 and fMet-tRNA from 20 nM (as used in the initial experiments) to a more physiologically relevant concentration<sup>58</sup> (1  $\mu$ M) resulted in an increase in the proportion of events with simultaneous IF2–GTP and fMet-tRNA binding; however, a significant proportion of both IF2-first and tRNA-first events was still observed<sup>57</sup>. As expected, omission of IF2 led to slow, unstable association of the 50S subunit. Thus, although IF2 and fMet-tRNA are required for rapid formation of the 70S ribosome, it seems that under physiological conditions there is no preference for either molecule to join the complex before the other. This result conflicts with the recent bulk-phase study of ribosome assembly, which found that although multiple assembly pathways are available, recruitment of each factor in the order IF3 > IF2 > IF1 > fMet-tRNA is kinetically favourable<sup>55</sup>. The reason for the discrepancy between the studies is unclear, but it should be noted that both experimental strategies have potential caveats. A complicating factor in the single-molecule experiment is that associations were measured in the context of nanoscale apertures within zero-mode waveguides<sup>57</sup>. Given the close proximity of the tethered molecules to the lower glass surface, the small size of these apertures (50–300 nm) and the relatively large size of the ribosome components (an assembled 70S ribosome has a diameter of 20 nm<sup>59</sup>), it is possible that diffusional access of some components into the compartments was hindered in some way, thus biasing the measured assembly rates. In the bulk-phase study, the preferred order of assembly was deduced from the average association and dissociation times of each individual initiation factor, when these factors were measured one at a time<sup>55</sup>. With this technique, it is not possible to directly quantify the

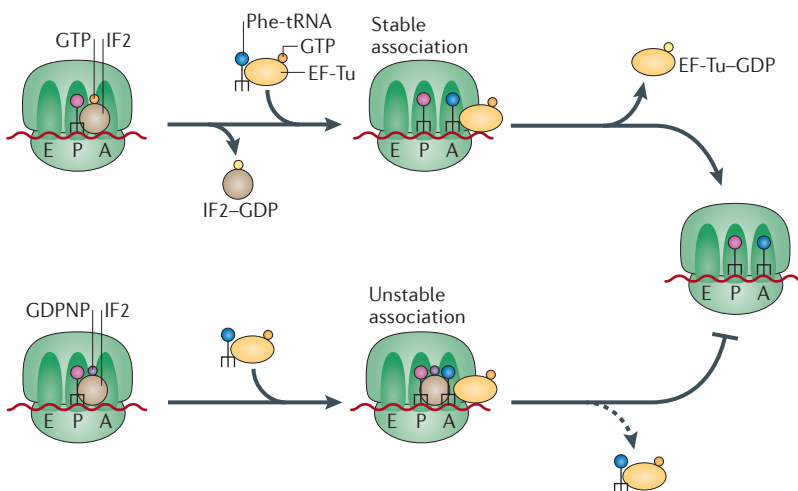
#### Zero-mode waveguides

Nanostructures that are used in microscopy; in these nanostructures, light is guided through compartments that are smaller than the wavelength of the light.

**a Initiation complex formation**



**b Binding of aminoacyl tRNA**



**c Translocation**

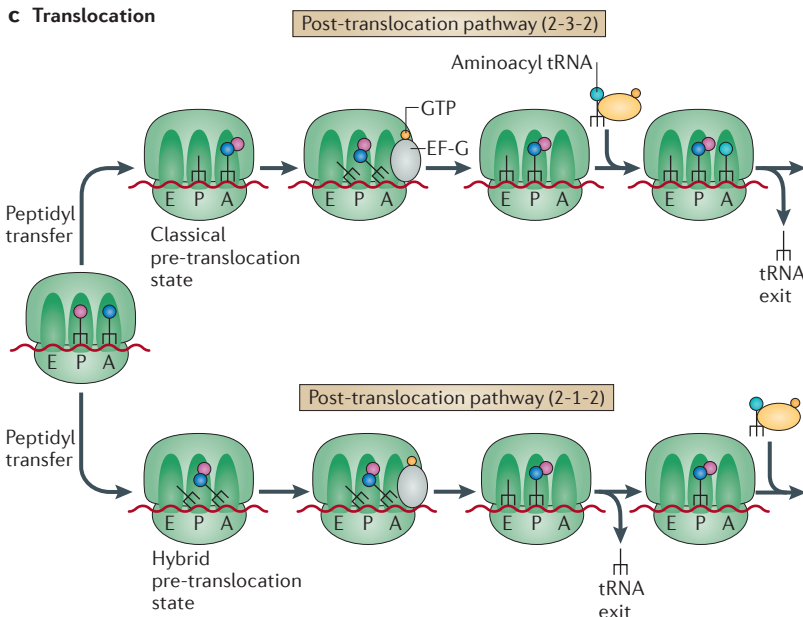


**Figure 4 | Monitoring translational events using a single-molecule approach.** The assembly of the 70S ribosome at the translation start site and the addition of elongator tRNAs are non-hierarchical events that can each occur through more than one pathway. **a** | The traditional view of initiation posits that translation initiation factor 2 (IF2)-GTP binds the initiator tRNA (N-formylmethionine (fMet)-bound tRNA<sup>fMet</sup> (fMet-tRNA)) and subsequently escorts it to the 30S ribosome subunit. However, multiwavelength fluorescence microscopy has shown that three alternative pathways are used: IF2-GTP can bind the 30S subunit first, the tRNA can bind first, or IF2-GTP and the initiator tRNA can bind simultaneously, as a complex<sup>57</sup>. **b** | The same study<sup>57</sup> used Förster (fluorescence) resonance energy transfer to show that during the next step, the first elongator tRNA can be delivered by elongation factor Tu (EF-Tu) before or, preferentially, after the departure of IF2 from the ribosome, but stable association of the tRNA with the ribosome requires that GTP is hydrolysed by IF2. Consistent with this, when the non-hydrolysable GTP analogue (GDPNP) is used, the association of Phe-tRNA is unstable (indicated by a dashed arrow). **c** | During the initial rounds of elongation, ribosomes follow one of two pathways for ejecting the deacylated tRNA from the E-site (exit site)<sup>62</sup>. In the newly uncovered 2-3-2 pathway, following translocation of the deacylated P-site (peptidyl site) tRNA to the E-site, this tRNA remains bound at the E-site until the incoming aminoacyl tRNA arrives at the A-site (acceptor site); thus, the ribosome progresses through states when two, then three, then two tRNAs are bound. In the previously known 2-1-2 pathway, the P-site tRNA is translocated to the E-site and exits the ribosome before the arrival of the next aminoacyl tRNA. Which pathway is followed depends on the geometry of the tRNAs at the time when elongation factor G (EF-G)-mediated translocation is enacted. Ribosomes in which the tRNAs adopt the hybrid pre-translocation state follow the 2-1-2 pathway. If, however, the tRNAs are in the classical pre-translocation state, the 2-3-2 pathway is followed.

proportion of assembly events that follow any particular pathway. Thus, further work is required to determine the relative importance of each pathway in the cellular environment.

After formation of the 70S initiation complex, the first non-initiator tRNA is escorted to the A-site by elongation factor Tu (EF-Tu). This step has also been visualized at the single-molecule level in real time<sup>57</sup>. The assembly pathway was monitored for labelled IF2-GTP (or IF2 in complex with the non-hydrolysable GTP analogue, GDPNP), labelled 50S subunit and labelled elongator tRNA (Phe-tRNA, in complex with EF-Tu-GTP) when added to the 30S subunit pre-loaded with both template mRNA and labelled fMet-tRNA (FIG. 4b). As expected, IF2 binding was quickly followed by 50S association. When IF2-GTP was used, Phe-tRNA formed a stable association with the complex, and its arrival usually coincided with IF2 departure. When IF2-GDPNP was used, only transient association of Phe-tRNA was observed, a phenomenon described as sampling (REFS 57,60). Collectively these observations point to a new checkpoint during the final stages of the initiation process: the first non-initiator tRNA can stably bind the

A-site only after the 50S subunit has joined and IF2 has hydrolysed GTP. One possibility is that this checkpoint has a role in the selection of cognate tRNA molecules. In the cellular environment, tRNA molecules (both cognate and non-cognate) would rapidly bind to and dissociate from the A-site of the ribosome before GTP hydrolysis on IF2. Only when the appropriate cognate tRNA is recognized would hydrolysis occur, leading to the release of IF2-GDP from the ribosome.

**A second pathway for tRNA exit during translocation.** During the elongation phase of translation, the peptidyl transferase reaction leads to transfer of the nascent peptide from the P-site tRNA to the A-site tRNA. The tRNAs must then be moved to facilitate binding of the next aminoacyl tRNA at the A-site; the newly deacylated tRNA in the P-site is moved to the E-site, and the aminoacyl tRNA occupying the A-site is moved to the P-site. This movement occurs in a process known as translocation, which is catalysed by elongation factor G (EF-G) in complex with GTP (FIG. 4c).

It is generally assumed that the deacylated tRNA rapidly and spontaneously dissociates from the E-site to facilitate subsequent rounds of elongation. However, the early rounds of elongation were recently examined using smFRET, and this uncovered an additional pathway of tRNA release that was not observed in later rounds of elongation<sup>61</sup>. In this pathway, the deacylated tRNA remains associated with the ribosomal E-site until the next charged tRNA binds to the A-site, at which point the deacylated tRNA is ejected from the E-site. This has been termed the 2-3-2 pathway, reflecting the fact that during the elongation cycle, either two or three tRNA molecules are always bound to the ribosome (FIG. 4c). In the first few cycles of elongation, both the 2-3-2 pathway and the more typical 2-1-2 pathway (in which the E-site tRNA is released before accommodation of the new A-site tRNA) are used. The choice of pathway was found to correlate with the particular conformational state adopted by the tRNA molecules during the pre-translocation stage. Those ribosomes in the so-called classical pre-translocation conformation (in which the A-site tRNA contacts the A-site on both the 30S and 50S subunits, referred to as A/A, and the P-site tRNA contacts the P-site on both the 30S and 50S subunits, referred to as P/P) almost always follow the 2-3-2 pathway. By contrast, those ribosomes in the hybrid state (in which the A-site tRNA contacts the A-site on the 30S subunit and the P-site on the 50S subunit, referred to as A/P, and the P-site tRNA contacts the P-site of the 30S subunit and the E-site of the 50S subunit, referred to as P/E) primarily follow the 2-1-2 pathway. The adoption of classical or hybrid geometry was stochastically determined in each round of translocation, so there is no correlation between 2-3-2 or 2-1-2 pathway usage in one round and the choice of pathway followed in the subsequent round.

### Perspectives

Recently, researchers at Stanford University (California, USA) and the J. Craig Venter Institute (Rockville, Maryland, USA) published the first computational

model of a complete bacterial cell, which simulated the growth of *Mycoplasma genitalium* at the level of individual molecules through multiple cell division cycles<sup>62</sup>. Although some of the fine details of this model will probably prove imperfect in the long run, the mere attempt to build such a model highlights just how much we now know about molecular processes in bacteria. The ultimate goal of a whole-cell model is to connect the actions of individual molecules to the phenotype of the cell. In this way, *in vitro* and *in vivo* single-molecule techniques used in combination are powerful tools for providing missing pieces of the puzzle. *In vitro* single-molecule studies are providing detailed kinetic information for biomolecular reactions and are proving invaluable for delineating complex, multiple-pathway systems. In parallel, *in vivo* single-molecule techniques are revealing how the actions of individual molecules are coordinated in the cellular environment and even how they can shape the phenotype of a whole cell<sup>28,30,63–65</sup>. Together, these two approaches are complimentary, as the *in vivo* measurements, although insightful, are far too complex to be interpreted in themselves and will always require reference to data measured in carefully controlled *in vitro* conditions for proper interpretation.

Despite the insight that has been gained from *in vitro* single-molecule studies, the list of unresolved questions within the fields of bacterial DNA replication, transcription and translation remains very long. The single-molecule approach, however informative, is not a cure-all solution. Single-molecule setups typically need to be tailored towards a specific type of measurement for a specific biological system, and a number of fundamental technical issues still exist. Fluorescence-based experiments, for example, are limited by the fact that when the concentration of a fluorescently labelled species exceeds ~1 nM, the signal from the surface-tethered molecules is completely obscured by background fluorescence, which is generated by unattached molecules free in solution. One approach to circumvent this problem involves immobilizing molecules within nanostructures called zero-mode waveguides<sup>57,60,66</sup>, an approach that allows physiologically relevant concentrations (in this case, micromolar concentrations) of fluorescent species to be analysed. There is, however, a physical size limit on the species that will fit into the apertures of these nanostructures (50–300 nm, corresponding to 150–1,000 bp of dsDNA), and there are substantial technical challenges associated with the production of these nanostructures. A recently reported alternative for imaging above the concentration barrier is to use photoswitchable fluorescent probes to selectively observe only those molecules bound to a tethered substrate<sup>67</sup>. This approach places no limit on the physical size of the system to be analysed, but requires a photoswitchable fluorescent probe and also that the species of interest forms a stable interaction (1 second or longer) with the tethered molecule. New approaches for imaging above the concentration barrier will probably be developed in the coming years, and together with advancements in other technologies, these new imaging techniques will help make the single-molecule approach compatible with a wider range of macromolecular complexes.

### Photoswitchable fluorescent probes

Molecules that change from being non-fluorescent to fluorescent, or vice versa, in response to light.

Interestingly, as single-molecule research has moved from the study of simple, one-protein systems into the study of complex processes like replication, transcription and translation, the lines between single-molecule biophysics and the traditional fields of biochemistry and microbiology have begun to blur. *In vitro* single-molecule studies now often encompass sophisticated biochemical strategies for preparing complex samples and stalling reactions in specific biochemical states<sup>68–73</sup>. At the same time, many biochemists are now regularly incorporating

single-molecule measurements into their studies<sup>34,74,75</sup>. Similar parallels can be drawn between molecular microbiology and *in vivo* single-molecule research, which is beginning to include the comparison of mutant strains in order to decode complex microscopy observations<sup>28,30,76,77</sup>. As new single-molecule techniques are developed and applied to study increasingly complex biological systems, there is little doubt that the single-molecule approach will continue to improve our understanding of the molecular mechanisms underlying fundamental processes in bacteria.

1. Bustamante, C., Cheng, W. & Mejia, Y. X. Revisiting the central dogma one molecule at a time. *Cell* **144**, 480–497 (2011).
2. Browning, D. F. & Busby, S. J. The regulation of bacterial transcription initiation. *Nature Rev. Microbiol.* **2**, 57–65 (2004).
3. Simonetti, A. *et al.* A structural view of translation initiation in bacteria. *Cell. Mol. Life Sci.* **66**, 423–436 (2009).
4. Thanbichler, M. Synchronization of chromosome dynamics and cell division in bacteria. *Cold Spring Harb. Perspect. Biol.* **2**, a000331 (2010).
5. Tinoco, I. Jr & Gonzalez, R. L. Jr. Biological mechanisms, one molecule at a time. *Genes Dev.* **25**, 1205–1231 (2011).
6. Moore, P. B. How should we think about the ribosome? *Annu. Rev. Biophys.* **41**, 1–19 (2012).  
**A review that asks a question of increasing importance in the molecular sciences: what is the most meaningful way to describe a molecular process?**
7. Dulin, D., Lipfert, J., Moolman, M. C. & Dekker, N. H. Studying genomic processes at the single-molecule level: introducing the tools and applications. *Nature Rev. Genet.* **14**, 9–22 (2012).  
**A review providing a detailed summary of the state-of-the-art tools for single-molecule experiments.**
8. Hamdan, S. M., Loparo, J. J., Takahashi, M., Richardson, C. C. & van Oijen, A. M. Dynamics of DNA replication loops reveal temporal control of lagging-strand synthesis. *Nature* **457**, 336–339 (2009).
9. Vanzi, F., Broggio, C., Sacconi, L. & Pavone, F. S. Lac repressor hinge flexibility and DNA looping: single molecule kinetics by tethered particle motion. *Nucleic Acids Res.* **34**, 3409–3420 (2006).
10. van Oijen, A. M. *et al.* Single-molecule kinetics of  $\lambda$  exonuclease reveal base dependence and dynamic disorder. *Science* **301**, 1235–1238 (2003).
11. Lipfert, J., Wiggin, M., Kerssemakers, J. W., Pedaci, F. & Dekker, N. H. Freely orbiting magnetic tweezers to directly monitor changes in the twist of nucleic acids. *Nature Commun.* **2**, 439 (2011).
12. Chen, C. *et al.* Single-molecule fluorescence measurements of ribosomal translocation dynamics. *Mol. Cell* **42**, 367–377 (2011).
13. Mott, M. L. & Berger, J. M. DNA replication initiation: mechanisms and regulation in bacteria. *Nature Rev. Microbiol.* **5**, 343–354 (2007).
14. Duderstadt, K. E., Chuang, K. & Berger, J. M. DNA stretching by bacterial initiators promotes replication origin opening. *Nature* **478**, 209–213 (2011).
15. Zorman, S., Seitz, H., Sclavi, B. & Strick, T. R. Topological characterization of the DnaA–*oriC* complex using single-molecule nanomanipulation. *Nucleic Acids Res.* **40**, 7375–7383 (2012).
16. Tanner, N. A. *et al.* *E. coli* DNA replication in the absence of free  $\beta$  clamps. *EMBO J.* **30**, 1830–1840 (2011).
17. Robinson, A. *et al.* Essential biological processes of an emerging pathogen: DNA replication, transcription, and cell division in *Acinetobacter* spp. *Microbiol. Mol. Biol. Rev.* **74**, 273–297 (2010).
18. Robinson, A., Causser, R. J. & Dixon, N. E. Architecture and conservation of the bacterial DNA replication machinery, an underexploited drug target. *Curr. Drug Targets* **13**, 352–372 (2012).
19. Soultanas, P. Loading mechanisms of ring helicases at replication origins. *Mol. Microbiol.* **84**, 6–16 (2012).
20. Zhang, Z. *et al.* Assembly of the bacteriophage T4 primosome: single-molecule and ensemble studies. *Proc. Natl Acad. Sci. USA* **102**, 3254–3259 (2005).
21. Smiley, R. D., Zhuang, Z., Benkovic, S. J. & Hammes, G. G. Single-molecule investigation of the T4 bacteriophage DNA polymerase holoenzyme: multiple pathways of holoenzyme formation. *Biochemistry* **45**, 7990–7997 (2006).
22. Tanner, N. A. *et al.* Real-time single-molecule observation of rolling-circle DNA replication. *Nucleic Acids Res.* **37**, e27 (2009).
23. Dixon, N. E. DNA replication: prime-time looping. *Nature* **462**, 854–855 (2009).
24. Manosas, M., Spiering, M. M., Zhuang, Z., Benkovic, S. J. & Croquette, V. Coupling DNA unwinding activity with primer synthesis in the bacteriophage T4 primosome. *Nature Chem. Biol.* **5**, 904–912 (2009).
25. Pandey, M. *et al.* Coordinating DNA replication by means of priming loop and differential synthesis rate. *Nature* **462**, 940–943 (2009).
26. Lee, J. B. *et al.* DNA primase acts as a molecular brake in DNA replication. *Nature* **439**, 621–624 (2006).
27. Jergic, S. *et al.* The unstructured C-terminus of the  $\tau$  subunit of *Escherichia coli* DNA polymerase III holoenzyme is the site of interaction with the  $\alpha$  subunit. *Nucleic Acids Res.* **35**, 2813–2824 (2007).
28. Lia, G., Michel, B. & Allemand, J. F. Polymerase exchange during Okazaki fragment synthesis observed in living cells. *Science* **335**, 328–331 (2012).
29. Loparo, J. J., Kulczyk, A. W., Richardson, C. C. & van Oijen, A. M. Simultaneous single-molecule measurements of phage T7 replisome composition and function reveal the mechanism of polymerase exchange. *Proc. Natl Acad. Sci. USA* **108**, 3584–3589 (2011).  
**An article describing a mechanism for core polymerase exchange at DNA replication forks, uncovered through a combination of force-based and fluorescence-based single-molecule methods.**
30. Johnson, D. E., Takahashi, M., Hamdan, S. M., Lee, S. J. & Richardson, C. C. Exchange of DNA polymerases at the replication fork of bacteriophage T7. *Proc. Natl Acad. Sci. USA* **104**, 5312–5317 (2007).
31. Reyes-Lamothe, R., Sherratt, D. J. & Leake, M. C. Stoichiometry and architecture of active DNA replication machinery in *Escherichia coli*. *Science* **328**, 498–501 (2010).
32. McInerney, P., Johnson, A., Katz, F. & O'Donnell, M. Characterization of a triple DNA polymerase replisome. *Mol. Cell* **27**, 527–538 (2007).
33. McHenry, C. S. DNA replicases from a bacterial perspective. *Annu. Rev. Biochem.* **80**, 403–436 (2011).
34. Georgescu, R. E., Kurth, I. & O'Donnell, M. E. Single-molecule studies reveal the function of a third polymerase in the replisome. *Nature Struct. Mol. Biol.* **19**, 113–116 (2012).
35. Gibb, B., Silverstein, T. D., Finkelstein, I. J. & Greene, E. C. Single-stranded DNA curtains for real-time single-molecule visualization of protein-nucleic acid interactions. *Anal. Chem.* **84**, 7607–7612 (2012).
36. Merrikh, H., Zhang, Y., Grossman, A. D. & Wang, J. D. Replication-transcription conflicts in bacteria. *Nature Rev. Microbiol.* **10**, 449–458 (2012).
37. Georgescu, R. E., Yao, N. Y. & O'Donnell, M. Single-molecule analysis of the *Escherichia coli* replisome and use of clamps to bypass replication barriers. *FEBS Lett.* **584**, 2596–2605 (2010).
38. Herbert, K. M., Greenleaf, W. J. & Block, S. M. Single-molecule studies of RNA polymerase: motoring along. *Annu. Rev. Biochem.* **77**, 149–176 (2008).
39. Larson, M. H., Landick, R. & Block, S. M. Single-molecule studies of RNA polymerase: one singular sensation, every little step it takes. *Mol. Cell* **41**, 249–262 (2011).
40. Kapanidis, A. N. *et al.* Initial transcription by RNA polymerase proceeds through a DNA-scrunching mechanism. *Science* **314**, 1144–1147 (2006).
41. Revyakina, A., Liu, C., Ebright, R. H. & Strick, T. R. Abortive initiation and productive initiation by RNA polymerase involve DNA scrunching. *Science* **314**, 1139–1143 (2006).
42. Frank, J. & Gonzalez, R. L. Jr. Structure and dynamics of a processive Brownian motor: the translating ribosome. *Annu. Rev. Biochem.* **79**, 381–412 (2010).
43. Yu, J. & Oster, G. A small post-translocation energy bias aids nucleotide selection in T7 RNA polymerase transcription. *Biophys. J.* **102**, 532–541 (2012).
44. Friedman, L. J. & Gelles, J. Mechanism of transcription initiation at an activator-dependent promoter defined by single-molecule observation. *Cell* **148**, 679–689 (2012).  
**A paper describing a single-molecule approach for monitoring the entire process of transcription initiation at a bacterial promoter.**
45. Kapanidis, A. N. *et al.* Retention of transcription initiation factor  $\sigma^{70}$  in transcription elongation: single-molecule analysis. *Mol. Cell* **20**, 347–356 (2005).
46. Cordes, T. *et al.* Sensing DNA opening in transcription using quenched Förster resonance energy transfer. *Biochemistry* **49**, 9171–9180 (2010).
47. Chakraborty, A. *et al.* Opening and closing of the bacterial RNA polymerase clamp. *Science* **337**, 591–595 (2012).
48. Sekine, S., Tagami, S. & Yokoyama, S. Structural basis of transcription by bacterial and eukaryotic RNA polymerases. *Curr. Opin. Struct. Biol.* **22**, 110–118 (2012).
49. Hartzog, G. A. & Kaplan, C. D. Competing for the clamp: promoting RNA polymerase processivity and managing the transition from initiation to elongation. *Mol. Cell* **43**, 161–163 (2011).
50. Tagami, S. *et al.* Crystal structure of bacterial RNA polymerase bound with a transcription inhibitor protein. *Nature* **468**, 978–982 (2010).
51. Aitken, C. E., Petrov, A. & Puglisi, J. D. Single ribosome dynamics and the mechanism of translation. *Annu. Rev. Biophys.* **39**, 491–513 (2010).
52. Blanchard, S. C. Single-molecule observations of ribosome function. *Curr. Opin. Struct. Biol.* **19**, 103–109 (2009).
53. Laursen, B. S., Sorensen, H. P., Mortensen, K. K. & Sperlberg-Petersen, H. U. Initiation of protein synthesis in bacteria. *Microbiol. Mol. Biol. Rev.* **69**, 101–123 (2005).
54. Milon, P. *et al.* The ribosome-bound initiation factor 2 recruits initiator tRNA to the 30S initiation complex. *EMBO Rep.* **11**, 312–316 (2010).
55. Milon, P., Maracci, C., Filonava, L., Gualerzi, C. O. & Rodnina, M. V. Real-time assembly landscape of bacterial 30S translation initiation complex. *Nature Struct. Mol. Biol.* **19**, 609–615 (2012).
56. Milon, P. & Rodnina, M. V. Kinetic control of translation initiation in bacteria. *Crit. Rev. Biochem. Mol. Biol.* **47**, 334–348 (2012).
57. Tsai, A. *et al.* Heterogeneous pathways and timing of factor departure during translation initiation. *Nature* **487**, 390–393 (2012).  
**An article that describes the assembly of the bacterial translation machinery as followed by single-molecule fluorescence microscopy.**
58. Caldas, T., Laalami, S. & Richarme, G. Chaperone properties of bacterial elongation factor EF-G and initiation factor IF2. *J. Biol. Chem.* **275**, 855–860 (2000).
59. Ban, N., Nissen, P., Hansen, J., Moore, P. B. & Steitz, T. A. The complete atomic structure of the large ribosomal subunit at 2.4 Å resolution. *Science* **289**, 905–920 (2000).

60. Uemura, S. *et al.* Real-time tRNA transit on single translating ribosomes at codon resolution. *Nature* **464**, 1012–1017 (2010).
61. Chen, C. *et al.* Allosteric versus spontaneous exit-site (E-site) tRNA dissociation early in protein synthesis. *Proc. Natl Acad. Sci. USA* **108**, 16980–16985 (2011).
62. Karr, J. R. *et al.* A whole-cell computational model predicts phenotype from genotype. *Cell* **150**, 389–401 (2012).  
**A report that describes the first computer model of the biochemical steps that occur during the bacterial cell cycle.**
63. Choi, P. J., Cai, L., Frieda, K. & Xie, X. S. A stochastic single-molecule event triggers phenotype switching of a bacterial cell. *Science* **322**, 442–446 (2008).
64. Li, G. W. & Xie, X. S. Central dogma at the single-molecule level in living cells. *Nature* **475**, 308–315 (2011).
65. Taniguchi, Y. *et al.* Quantifying *E. coli* proteome and transcriptome with single-molecule sensitivity in single cells. *Science* **329**, 533–538 (2010).
66. Levene, M. J. *et al.* Zero-mode waveguides for single-molecule analysis at high concentrations. *Science* **299**, 682–686 (2003).
67. Loveland, A. B., Habuchi, S., Walter, J. C. & van Oijen, A. M. A general approach to break the concentration barrier in single-molecule imaging. *Nature Methods* **9**, 987–992 (2012).
68. Aitken, C. E. & Puglisi, J. D. Following the intersubunit conformation of the ribosome during translation in real time. *Nature Struct. Mol. Biol.* **17**, 793–800 (2010).
69. Altıntop, M. E., Ly, C. T. & Wang, Y. Single-molecule study of ribosome hierarchic dynamics at the peptidyl transferase center. *Biophys. J.* **99**, 3002–3009 (2010).
70. Feldman, M. B., Terry, D. S., Altman, R. B. & Blanchard, S. C. Aminoglycoside activity observed on single pre-translocation ribosome complexes. *Nature Chem. Biol.* **6**, 54–62 (2010).
71. Ly, C. T., Altıntop, M. E. & Wang, Y. Single-molecule study of viomycin's inhibition mechanism on ribosome translocation. *Biochemistry* **49**, 9732–9738 (2010).
72. Munro, J. B., Wasserman, M. R., Altman, R. B., Wang, L. & Blanchard, S. C. Correlated conformational events in EF-G and the ribosome regulate translocation. *Nature Struct. Mol. Biol.* **17**, 1470–1477 (2010).
73. Wang, L. *et al.* Allosteric control of the ribosome by small-molecule antibiotics. *Nature Struct. Mol. Biol.* **19**, 957–963 (2012).
74. Nelson, S. W. & Benkovic, S. J. Response of the bacteriophage T4 replisome to noncoding lesions and regression of a stalled replication fork. *J. Mol. Biol.* **401**, 743–756 (2010).
75. Yao, N. Y., Georgescu, R. E., Finkelstein, J. & O'Donnell, M. E. Single-molecule analysis reveals that the lagging strand increases replisome processivity but slows replication fork progression. *Proc. Natl Acad. Sci. USA* **106**, 13236–13241 (2009).
76. Badrinarayanan, A., Reyes-Lamothe, R., Uphoff, S., Leake, M. C. & Sherratt, D. J. *In vivo* architecture and action of bacterial structural maintenance of chromosome proteins. *Science* **338**, 528–531 (2012).
77. Lia, G. *et al.* RecA-promoted, RecFOR-independent progressive disassembly of replisomes stalled by helicase inactivation. *Mol. Cell* **49**, 547–557 (2012).
78. Etsen, C. M., Hamdan, S. M., Richardson, C. C. & van Oijen, A. M. Thioredoxin suppresses microscopic hopping of T7 DNA polymerase on duplex DNA. *Proc. Natl Acad. Sci. USA* **107**, 1900–1905 (2010).
79. Sinha, N. K., Morris, C. F. & Alberts, B. M. Efficient *in vitro* replication of double-stranded DNA templates by a purified T4 bacteriophage replication system. *J. Biol. Chem.* **255**, 4290–4293 (1980).
80. Qu, X. *et al.* The ribosome uses two active mechanisms to unwind messenger RNA during translation. *Nature* **475**, 118–121 (2011).
81. Tang, G. Q., Roy, R., Bandwar, R. P., Ha, T. & Patel, S. S. Real-time observation of the transition from transcription initiation to elongation of the RNA polymerase. *Proc. Natl Acad. Sci. USA* **106**, 22175–22180 (2009).

#### Acknowledgements

A.M.v.O. is supported by grants from the Netherlands Organisation for Scientific Research (NWO; Vici 680-47-607) and the European Research Council (ERC 281098).

#### Competing interests statement

The authors declare no competing financial interests.

#### FURTHER INFORMATION

Andrew Robinson and Antoine M. van Oijen's homepage: <http://www.singlemolecule.nl>

ALL LINKS ARE ACTIVE IN THE ONLINE PDF